Journal of Fluids and Structures 86 (2019) 0–12

Contents lists available at ScienceDirect

Journal of Fluids and Structures

journal homepage: www.elsevier.com/locate/jfs

Flutter prediction methodology based on dynamic eigen decomposition and frequency-domain stability

Taehyoun Kim

Pegase Avtech, Bothell, WA, USA

ARTICLE INFO

Article history:
Received 7 January 2018
Received in revised form 23 September 2018
Accepted 23 January 2019
Available online xxxx

Keywords:
Flutter
Aeroelasticity
Dynamic Eigen Decomposition (DED)
Dynamic eigenvalues and eigenmodes
Nyquist stability
Frequency domain

ABSTRACT

In this work, based on the concept of the Dynamic Eigen Decomposition and the frequency domain stability criterion a new flutter theory and methodology are presented. It is shown that the dynamic eigenmodes of the aeroelastic system can be formulated such that they become an intrinsic property independent of dynamic pressure. Hence, it is possible to predict the aeroelastic instability by a simple extrapolation of the corresponding dynamic eigenvalues obtained at a low dynamic pressure without the need for the p–k iterations, the k iterations, or the p iterations, all of which require computationally expensive and numerically sensitive procedures. The proposed scheme is demonstrated using Goland wing modeled by a finite element and doublet lattice. It is shown that under the restriction of constant Mach, varying altitude and a mean air speed the new approach yields a mathematically exact flutter solution which includes the flutter mode shape as well as the critical dynamic pressure and frequency.

1. Introduction

Flutter is a well-known mechanism by which air vehicles become dynamically unstable through the interaction of the fluid forces and elastic deformation of the structure. It is a dangerous phenomenon to be avoided during the design, analysis, and tests of all aircraft structures. Although there exist tools that enable estimating analytically the onset of the aeroelastic instability, they are often computationally expensive and numerically sensitive. Typically, a flutter calculation is done in the mixed time–frequency domain; the structural dynamics is described by the generalized mass, stiffness, and damping matrices, while the unsteady aerodynamics is represented by the complex valued matrix called the generalized aerodynamic force (GAF) matrix in frequency domain. Since aeroelastic damping and frequency information is not known a priori in this mixed formulation, an iterative algorithm must be implemented and executed to track every aeroelastic mode as a function of air speed or dynamic pressure and the frequency. When the damping of any mode becomes zero it defines the condition of flutter. For example, the p–k method (Winther et al., 2000) which is the standard flutter method in aeronautical industry nowadays requires mode tracking, a secondary process that could run into a divergence due to potentially discontinuous nature of the aeroelastic modes. This is particularly a concerning issue when dealing with an aircraft model that has

E-mail address: johnkim@pegaseavtech.com.

https://doi.org/10.1016/j.jfluidstructs.2019.01.022
0889-9746/

Nomenclature

$\boldsymbol{A}, \boldsymbol{B}, \boldsymbol{C}$	linear system or aeroelastic system matrices
$\boldsymbol{A}_0, \boldsymbol{B}_0, \boldsymbol{C}_0$	nominal system matrices
$\boldsymbol{A}_a, \boldsymbol{B}_a, \boldsymbol{C}_a, \boldsymbol{D}_a$	aerodynamic system matrices
$\boldsymbol{A}_s, \boldsymbol{B}_s, \boldsymbol{B}_i, \boldsymbol{C}_s$	structural system matrices
$\boldsymbol{\Delta A}$	perturbed incremental system matrix
b	reference length (ft)
$\boldsymbol{G}(\omega)$	transfer function matrix of perturbed system
h	altitude (ft)
k	reduced frequency ($\equiv \frac{\omega b}{V_\infty}$) or a scalar gain
L	dimension of aeroelastic system ($= 2N + M$)
M	number of aerodynamic states
M_∞	Mach number
$\boldsymbol{M}, \boldsymbol{C}, \boldsymbol{K}$	generalized mass, damping, stiffness matrices
N	number of structural states or modes
q_D	dynamic pressure ($\equiv \frac{1}{2}\rho_\infty V_\infty^2$) ($\frac{slug}{\text{ft s}^2}$)
$\boldsymbol{q}$	($N \times 1$) generalized structural coordinates vector
$\boldsymbol{Q}$	generalized aerodynamic force (GAF) matrix
$\boldsymbol{T}(\omega)$	system transfer matrix
$\boldsymbol{u}$	system inputs vector
$\boldsymbol{v}(\omega)$, $\boldsymbol{w}(\omega)$	right and left dynamic eigenvector
V_∞	free stream air speed ($\frac{\text{ft}}{\text{s}}$)
$\boldsymbol{V}(\omega)$, $\boldsymbol{W}(\omega)$	right and left dynamic eigenvector matrices
$\boldsymbol{x}$	($M \times 1$) aerodynamic states vector
$\boldsymbol{X}$	($L \times 1$) aeroelastic states vector
$\boldsymbol{X}_0$	nominal solution of $\boldsymbol{X}$
$\boldsymbol{\Delta X}$	perturbed solution of $\boldsymbol{X}$
$\boldsymbol{y}$	aerodynamic loads vector
$\boldsymbol{z}$	($2N \times 1$) structural states vector
ρ_∞	air density ($\frac{slug}{\text{ft}^3}$)
λ	dynamic eigenvalue
$\boldsymbol{\Lambda}(\omega)$	dynamic eigenvalue matrix
ω	frequency ($\frac{\text{rad}}{\text{s}}$)

a complicated configuration and requires many structural modes to include. The Rational Function Approximation (RFA) circumvents this difficulty by fitting the complex valued aerodynamic loads in terms of zeros and poles, putting it in a state-space form (Roger, 1977; Karpel, 1982). Once the structural and aerodynamic matrices are put together, the continuous-time, state-space aeroelastic matrix can be solved to produce eigenvalues and from them the aeroelastic instability can be determined. The downsides, however, are the augmented size of the equation and the approximation of the unsteady aerodynamics which could lead to inaccurate flutter solutions.

Most recently, Kim (2015, 2016), Kim and Dowell (2017), Kim (2018) introduced the Dynamic Eigen Decomposition (DED) in obtaining parametrically rich solution subspaces for linear and nonlinear systems. The idea is to express the general solution as a superposition of convolutions between the *dynamic eigenmodes* $\boldsymbol{v}_i(t)$'s and generalized coordinates $a_i(t)$'s:

$$\boldsymbol{x}(t) = \boldsymbol{v}_1 * a_1 + \boldsymbol{v}_2 * a_2 \ldots + \boldsymbol{v}_R * a_R \tag{1}$$

where $*$ denotes the time convolution. By allowing the eigenmodes to be *time-varying* and convoluting them with the coordinates it broadens the range of the modal space, thereby capturing the continuous parameter variations and the varying degrees of the nonlinearities. Much like the conventional eigenvalue problem, the dynamic eigenmodes are associated with *dynamic eigenvalues,* $\lambda_i(\omega)$'s:

$$\boldsymbol{T}(\omega)\boldsymbol{v}_i(\omega) = \lambda_i(\omega)\,\boldsymbol{v}_i(\omega) \tag{2}$$

for a properly defined frequency valued square matrix $\boldsymbol{T}(\omega)$. The goal of the DED is then to use the single set of the modes $\boldsymbol{v}_i(\omega)$'s for all the variations in the parameters and nonlinearities.

In the present work, a new flutter prediction scheme is formulated based on the DED such that the aeroelastic stability can be determined by checking the dynamic eigenvalues $\lambda_i(\omega)$'s in frequency domain. It will be shown that a flutter instability

is entirely determined by extrapolating a single dynamic eigenvalue obtained at any dynamic pressure through a scalar gain factor, and hence it is possible to avoid the computationally expensive and sensitive procedures mentioned earlier. Another key finding of the work is that flutter can be viewed as an intrinsic property of the aeroelastic system rather than a particular solution at the dynamic instability because the critical flutter mode identified is independent of dynamic pressure.

2. Dynamic Eigen Decomposition (DED) of aeroelastic system

In this section, the DED that leads to the new aeroelastic stability equation and criterion is introduced. Towards this end, we will rely on the so called statically nonlinear, dynamically linearized (SNLDL) modeling in which nonlinearities are allowed in the static part of the model but the dynamic part is linearized about the nonlinear static solution to yield a small amplitude, linearized oscillation. Apart from the SNLDL requirement for the linear flutter analysis, the stability criterion we will derive is generic and applicable to any type of aeroelastic models. Following the notations of Kim (2016), we will assume that a linear structural dynamic system can be described by N structural modes given in discrete-time, state-space as

$$\boldsymbol{z}^{n+1} = \boldsymbol{A}_s \boldsymbol{z}^n + \boldsymbol{B}_s \boldsymbol{y}^n + \boldsymbol{B}_i \boldsymbol{u}^n \tag{3}$$

Similarly, an aerodynamic system in M states is given by

$$\begin{aligned} \boldsymbol{x}^{n+1} &= \boldsymbol{A}_a \boldsymbol{x}^n + \boldsymbol{B}_a \boldsymbol{z}^n \\ \boldsymbol{y}^n &= q_D \left(\boldsymbol{C}_a \boldsymbol{x}^n + \boldsymbol{D}_a \boldsymbol{z}^n \right) \end{aligned} \tag{4}$$

According to the SNLDL assumption, aerodynamic nonlinearities such as a transonic shock can be included in (4) but only in the static sense. Using the equations, one can write a coupled fluid–structure equation of motion subject to *varying dynamic pressure but at a constant Mach number* as follows:

$$\boldsymbol{X}^{n+1} = \boldsymbol{A}\left(q_D\right) \boldsymbol{X}^n + \boldsymbol{B}\boldsymbol{u}^n \tag{5}$$

where

$$\begin{aligned} \boldsymbol{X} &\equiv \left\{ \begin{array}{c} \boldsymbol{x} \\ \boldsymbol{z} \end{array} \right\} \\ \boldsymbol{A}\left(q_D\right) &\equiv \left[\begin{array}{cc} \boldsymbol{A}_a & \boldsymbol{B}_a \\ q_D \boldsymbol{B}_s \boldsymbol{C}_a & \boldsymbol{A}_s + q_D \boldsymbol{B}_s \boldsymbol{D}_a \end{array} \right], \boldsymbol{B} \equiv \left[\begin{array}{c} 0 \\ \boldsymbol{B}_i \end{array} \right] \end{aligned} \tag{6}$$

Let us divide the aeroelastic states vector $\boldsymbol{X}$ into *nominal* and *perturbed* parts

$$\boldsymbol{X} = \boldsymbol{X}_0 + \Delta \boldsymbol{X} \tag{7}$$

where $\boldsymbol{X}_0$ and $\Delta \boldsymbol{X}$ beach satisfies,

$$\boldsymbol{X}_0^{n+1} = \boldsymbol{A}\left(q_{D0}\right) \boldsymbol{X}_0^n + \boldsymbol{B}\boldsymbol{u}^n \text{ : Nominal} \tag{8}$$

$$\Delta \boldsymbol{X}^{n+1} = \boldsymbol{A}\left(q_D\right) \Delta \boldsymbol{X}^n + \Delta \boldsymbol{A} \boldsymbol{X}_0^n \text{ : Perturbed} \tag{9}$$

where $\Delta \boldsymbol{A} \equiv \Delta q_D \overline{\Delta \boldsymbol{A}}$, $\Delta q_D \equiv q_D - q_{D0}$ and

$$\overline{\Delta \boldsymbol{A}} \equiv \left[\begin{array}{cc} 0 & 0 \\ \boldsymbol{B}_s \boldsymbol{C}_a & \boldsymbol{B}_s \boldsymbol{D}_a \end{array} \right] = Const \tag{10}$$

In the above derivation, two underlying assumptions are:

1. Nominal aeroelastic system (8) is stable.
2. Along the Constant Mach, Varying Altitude (CMVA) air speed is fixed and only density changes.

When altitude is varied the speed of sound also changes with the altitude. However, as can be seen in Fig. 1, in the range of (0, 200,000) ft the variation in the speed of sound is within +9% and − 5.5% from its mean value, 1023.7 ft/s. Furthermore, of the two terms in the local downwash $\alpha + \dot{h}/V$ that determines the unsteady pressures on the lifting surface this change in the air speed influences the local plunging $\dot{h}/V$ but not the local pitching α, and as such the percentage change in the aerodynamic loads due to the speed change will be smaller. Thus, when the so-called matched point solution is sought one may assume that the airplane speed is fixed along the CMVA line. Based on this assumption, flutter is determined by the dynamic instability of the perturbed system, Eq. (9).

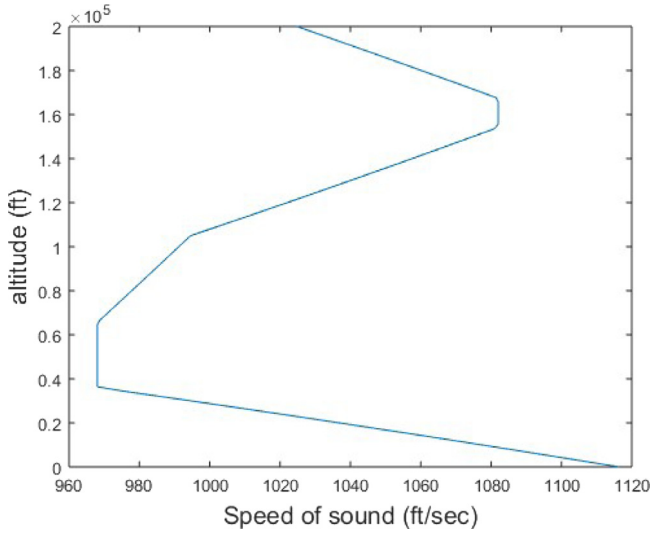

Fig. 1. Altitude vs. speed of sound of standard atmosphere.

Assuming a sinusoidal solution in the form, $\boldsymbol{\Delta X}^n(\omega) \equiv \overline{\boldsymbol{\Delta X}} e^{j\omega n\Delta t}$ (Δt = an incremental time) (9) can be rewritten in frequency domain,

$$\overline{\boldsymbol{\Delta X}} e^{j\omega(n+1)\Delta t} = \boldsymbol{A}(q_D)\,\overline{\boldsymbol{\Delta X}} e^{j\omega n\Delta t} + \boldsymbol{\Delta A}\overline{\boldsymbol{X}}_0 e^{j\omega n\Delta t} \tag{11}$$

from which the transfer function of the perturbed equation from $\overline{\boldsymbol{X}}_0$ to $\overline{\boldsymbol{\Delta X}}$ becomes

$$\boldsymbol{G}(\omega) \equiv [z\boldsymbol{I} - \boldsymbol{A}(q_D)]^{-1}\,\boldsymbol{\Delta A} \tag{12}$$

where $z \equiv e^{j\omega\Delta t}$. Now, take an eigen decomposition of the transfer function:

$$\boldsymbol{G}(\omega) = [z\boldsymbol{I} - \boldsymbol{A}(q_D)]^{-1}\,\boldsymbol{\Delta A} \equiv \boldsymbol{V}_\nu(\omega)\,\boldsymbol{\Lambda}_\nu(\omega)\,\boldsymbol{W}_\nu^T(\omega) \tag{13}$$

where

$\nu \equiv rank(\boldsymbol{G}(\omega)) = rank\left(\overline{\boldsymbol{\Delta A}}\right) = 2N$
$\boldsymbol{\Lambda}_\nu = (\nu \times \nu)$ diagonal matrix with nonzero dynamic eigenvalues
$\boldsymbol{V}_\nu, \boldsymbol{W}_{\boldsymbol{\nu}} =$ matrices of right and left dynamic eigenvectors
$\boldsymbol{V}_\nu(\omega)\boldsymbol{W}_\nu^\dagger(\omega) = \boldsymbol{I}_\nu$ *(orthonormality)*

Note that although we started out with the full-order coupled fluid–structure Eq. (5), we find that there are only ν nonzero eigenvalues and hence ν eigenvectors, exactly twice the number of structural degrees of freedom, that determine the aeroelastic instability. It can be shown that the following transfer function is '*modally equivalent*' to (13) (Kim, 2015).

$$\boldsymbol{G}'(\omega) \equiv [z\boldsymbol{I} - \boldsymbol{A}(q_{D0})]^{-1}\,\boldsymbol{\Delta A} \equiv \boldsymbol{V}'_\nu(\omega)\,\boldsymbol{\Lambda}'_\nu(\omega)\,\boldsymbol{W}_\nu^{T'}(\omega) \tag{14}$$

with

$$\boldsymbol{V}'_\nu(\omega) \equiv \boldsymbol{V}_\nu(\omega),\ \boldsymbol{W}'_\nu(\omega) \equiv \boldsymbol{W}_\nu(\omega) \tag{15}$$

That is, (13) and (14) share the same set of dynamic eigenmodes, $\boldsymbol{V}_\nu(\omega)$ and $\boldsymbol{W}_\nu(\omega)$, and the dynamic eigenvalues at the two parameters, q_{D0} and q_D, are related to each other as

$$\boldsymbol{\Lambda}'_\nu(\omega) \equiv [\boldsymbol{I}_\nu + \boldsymbol{\Lambda}_\nu(\omega)]^{-1}\boldsymbol{\Lambda}_\nu(\omega) \tag{16}$$

It should be emphasized that the eigenvectors and eigenvalues used in the above derivation of the modal equivalence are *dynamic* in that they are not constant but are continuous functions of frequency or time. That they are different from the traditional system eigenvalues and vectors, i.e., the solutions of $\boldsymbol{Av} = \lambda\boldsymbol{v}$, becomes obvious if one converts the frequency domain equations to time domain. Letting $\boldsymbol{V}_\nu(t)$, $\boldsymbol{\Lambda}_\nu(t)$, $\boldsymbol{\Lambda}'_{\boldsymbol{\nu}}(t)$, $\boldsymbol{W}_\nu^T(t)$ denote the inverse Fourier transforms of $\boldsymbol{V}_\nu(\omega)$, $\boldsymbol{\Lambda}_\nu(\omega)$, $\boldsymbol{\Lambda}'_{\boldsymbol{\nu}}(\omega)$, $\boldsymbol{W}_\nu^T(\omega)$, the time domain solutions to (13) and (14) are

$$\boldsymbol{G}(t) = \int_0^t \boldsymbol{V}_\nu(t-\tau_2)\left[\int_0^{\tau_2} \boldsymbol{\Lambda}_\nu(\tau_2-\tau_1)\,\boldsymbol{W}_\nu^T(\tau_1)\,d\tau_1\right]d\tau_2 \tag{17}$$

$$\boldsymbol{G}'(t) = \int_0^t \boldsymbol{V}_\nu(t-\tau_2)\left[\int_0^{\tau_2} \boldsymbol{\Lambda}'_{\boldsymbol{\nu}}(\tau_2-\tau_1)\,\boldsymbol{W}_\nu^T(\tau_1)\,d\tau_1\right]d\tau_2 \tag{18}$$

That is, the system responses are expressed as time convolutions between the dynamic eigenvectors and eigenvalues and hence include all the causal effects accumulated from the beginning to the present time. The conventional system eigenvectors do not allow such an expression for the system response as they do not have the temporal memory effects.

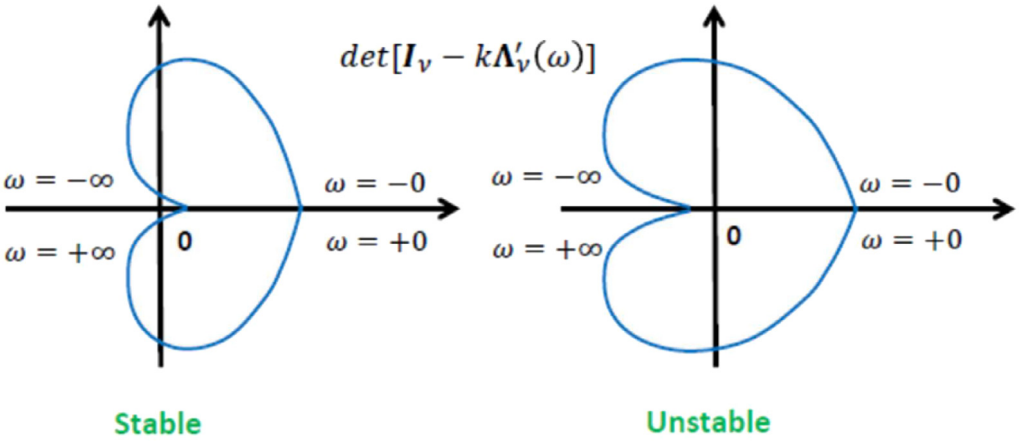

Fig. 2. Stable and unstable Multi-Input Multi-Output (MIMO) systems according to Nyquist Stability.

3. Stability of coupled aeroelastic systems based on dynamic eigenvalues

Suppose the dynamic pressure is increased by $k\Delta q_D$ instead of Δq_D from the nominal q_{D0}. Then the new $\boldsymbol{G}(\omega)$ will be modally equivalent to

$$\boldsymbol{G}'(\omega) = [z\boldsymbol{I} - \boldsymbol{A}(q_{D0})]^{-1} k\boldsymbol{\Delta A} \equiv \boldsymbol{V}_\nu(\omega)\, k\boldsymbol{\Lambda}'_\nu(\omega)\, \boldsymbol{W}_\nu^T(\omega) \tag{19}$$

which has new eigenvalues $k\lambda'_{\nu i}(\omega)$ but retains the same eigenvectors. Hence, the dynamic eigenvalues of the new perturbed system are expressed as

$$\boldsymbol{\Lambda}_\nu(\omega) \equiv [\boldsymbol{I}_\nu - k\boldsymbol{\Lambda}'_\nu(\omega)]^{-1} k\boldsymbol{\Lambda}'_\nu(\omega) \tag{20}$$

Since $\boldsymbol{v}_{\nu i}(t)$'s, $\boldsymbol{w}_{\nu i}(t)$'s are invariant under $k\Delta q_D$ and their magnitudes are bounded by the orthonormality, the stability of the transfer function and therefore the flutter boundary will be determined by $\boldsymbol{\lambda}_{\nu i} = \frac{k\lambda'_{\nu i}}{1-k\lambda'_{\nu i}} (i = 1, 2, \ldots \nu)$. Invoking the Multi-Input Multi-Output (MIMO) Nyquist Stability Theorem (Maciejowski, 1989), one can make the following statement about the stability of the aeroelastic system:

"Based on (20), for a stable aeroelastic equation of motion (5) undergoing a change in dynamic pressure the Nyquist plot of $det[\boldsymbol{I}_\nu - k\boldsymbol{\Lambda}'_\nu(\omega)]$ must not encircle the origin of the complex plane". (See Fig. 2.)

When applying the frequency domain stability to the aeroelastic system at hand, one can expect that the values of $(k_f,\ \omega_f)$ that make $det\left[\boldsymbol{I}_\nu - k_f\boldsymbol{\Lambda}'_\nu(\omega_f)\right]$ just vanish define the condition of flutter and $q_{D0} + k_f\Delta q_D$ becomes the critical dynamic pressure. Equivalently, at least one of $k_f\lambda'_{\nu i}(\omega_f)$ $(i = 1, 2 \ldots \nu)$ will touch the unity at the flutter. Apart from the critical dynamic pressure and frequency, the Nyquist plot itself does not reveal the flutter mode, nor aeroelastic damping and frequency information away from the flutter. However, as will be proved in the next section the flutter mode is identified as the corresponding dynamic eigenvector $\boldsymbol{v}_{\nu i}(\omega)$ at $\omega = \omega_f$.

4. Identification of flutter mode as a dynamic eigenmode

At the flutter (ω_k, q_{Dk}) the matrix of the perturbed equation (13) becomes singular with zero damping. Hence, we expect

$$det|z_f\boldsymbol{I} - \boldsymbol{A}(q_{Df})| = 0 \tag{21}$$

where $z_f \equiv e^{j\omega_f \Delta t}$. It implies that one of $\lambda_\nu(\omega_f)$'s must diverge. So, let $\lambda_{\nu 1}(\omega_f) \to \infty$. Multiplying both sides of (13) at the flutter condition with $z_f\boldsymbol{I} - \boldsymbol{A}(q_{Df})$ we get

$$\begin{aligned} q_{Df}\overline{\boldsymbol{\Delta A}} &\equiv [z_f\boldsymbol{I} - \boldsymbol{A}(q_{Df})]\boldsymbol{V}_\nu(\omega_f)\,\boldsymbol{\Lambda}_\nu(\omega_f)\,\boldsymbol{W}_\nu^T(\omega_f) \\ &= \left[z_f\boldsymbol{I} - \boldsymbol{A}(q_{Df})\right]\left[\boldsymbol{v}_{\nu 1}(\omega_f)\,\lambda_{\nu 1}(\omega_f)\,\boldsymbol{w}_{\nu 1}^T(\omega_f) + \sum_{i=2}^{\nu} \boldsymbol{v}_{\nu i}(\omega_f)\,\lambda_{\nu i}(\omega_f)\,\boldsymbol{w}_{\nu i}^T(\omega_f)\right] \end{aligned} \tag{22}$$

Since the left-hand side is finite and $\lambda_{\nu 1}(\omega_f) \to \infty$, we must require

$$\left[z_f\boldsymbol{I} - \boldsymbol{A}(q_{Df})\right]\boldsymbol{v}_{\nu 1}(\omega_f) = 0 \tag{23}$$

because otherwise the first term in the right-hand side of (22) will diverge. Therefore, by Eq. (23) and the definition of flutter we conclude that $\boldsymbol{v}_{\nu 1}(\omega_f)$ is the flutter mode. This result suggests that the flutter mode which is invariant under all Δq_D's and k's could be viewed as *an intrinsic property* of the aeroelastic system, rather than a solution at the particular condition.

5. Flutter prediction based on structural measurements

Recalling $\boldsymbol{G}(\omega)$ is the transfer function from $\boldsymbol{X}_0$ to $\boldsymbol{\Delta X} = \boldsymbol{X} - \boldsymbol{X}_0$, (13) can be rewritten:

$$\boldsymbol{G}(\omega) = [z\boldsymbol{I} - \boldsymbol{A}(q_D)]^{-1}\,\boldsymbol{\Delta A} = \boldsymbol{T}(\omega)\,\boldsymbol{T}_0^{-1}(\omega) - \boldsymbol{I} \tag{24}$$

where

$$\boldsymbol{T}_0(\omega) = [z\boldsymbol{I} - \boldsymbol{A}(q_{D0})]^{-1} \tag{25}$$

$$\boldsymbol{T}(\omega) = [z\boldsymbol{I} - \boldsymbol{A}(q_D)]^{-1} \tag{26}$$

are the transfer function matrices of the system at q_{D0} and q_D, respectively. Focusing on the ν nonzero eigenvalues, let us examine the following $(2N \times 2N)$ transfer function matrix

$$\boldsymbol{G}_z(\omega) = \boldsymbol{C}\,[z\boldsymbol{I} - \boldsymbol{A}(q_D)]^{-1}\,\boldsymbol{B}\left[\boldsymbol{C}\,[z\boldsymbol{I} - \boldsymbol{A}(q_{D0})]^{-1}\,\boldsymbol{B}\right]^{-1} - \boldsymbol{I}_\nu \tag{27}$$

where

$$\boldsymbol{B} = \begin{bmatrix} 0(M \times \nu) \\ \boldsymbol{B}_\nu(\nu \times \nu) \end{bmatrix},\ \boldsymbol{C} = \begin{bmatrix} 0(\nu \times M) & \boldsymbol{C}_\nu(\nu \times \nu) \end{bmatrix} \tag{28}$$

$\boldsymbol{B}_\nu, \boldsymbol{C}_\nu$ can be fully populated and arbitrary. Note only the structural degrees of freedom are directly excited by $\boldsymbol{B}$ and only the structural responses are sampled by $\boldsymbol{C}$. For such a matrix $\boldsymbol{B}$, $\boldsymbol{\Delta A}\cdot(\boldsymbol{\Delta A}^{-p}\boldsymbol{B})$ does not vanish and is equal to $\boldsymbol{B}$ ($-p$ denotes pseudo inverse). Hence, one can rewrite (27) as

$$\begin{aligned}
\boldsymbol{G}_z(\omega) &= \boldsymbol{C}\,[z\boldsymbol{I} - \boldsymbol{A}(q_D)]^{-1}\,\boldsymbol{\Delta A}\cdot(\boldsymbol{\Delta A}^{-p}\boldsymbol{B}) \\
&\quad\cdot\left[\boldsymbol{C}\,[z\boldsymbol{I} - \boldsymbol{A}(q_{D0})]^{-1}\,\boldsymbol{\Delta A}\cdot(\boldsymbol{\Delta A}^{-p}\boldsymbol{B})\right]^{-1} - \boldsymbol{I}_\nu \\
&= \boldsymbol{C}\boldsymbol{V}_\nu(\omega)\,\boldsymbol{\Lambda}_\nu(\omega)\,\boldsymbol{W}_\nu^T(\omega)\,(\boldsymbol{\Delta A}^{-p}\boldsymbol{B}) \\
&\quad\cdot\left[\boldsymbol{C}\boldsymbol{V}_\nu(\omega)\,\boldsymbol{\Lambda}'_\nu(\omega)\,\boldsymbol{W}_\nu^T(\omega)\,(\boldsymbol{\Delta A}^{-p}\boldsymbol{B})\right]^{-1} - \boldsymbol{I}_\nu \\
&\equiv \boldsymbol{C}_\nu(\omega)\,\boldsymbol{\Lambda}_\nu(\omega)\,\boldsymbol{B}_\nu(\omega)\,[\boldsymbol{C}_\nu(\omega)\,\boldsymbol{\Lambda}'_\nu(\omega)\,\boldsymbol{B}_\nu(\omega)]^{-1} - \boldsymbol{I}_\nu
\end{aligned} \tag{29}$$

where

$$\begin{aligned}
\boldsymbol{B}_\nu(\omega) &\equiv \boldsymbol{W}_\nu^T(\omega)\left(\boldsymbol{\Delta A}^{-p}\boldsymbol{B}\right)\ (\nu \times \nu) \\
\boldsymbol{C}_\nu(\omega) &\equiv \boldsymbol{C}\boldsymbol{V}_\nu(\omega)\,(\nu \times \nu)
\end{aligned} \tag{30}$$

Since $\boldsymbol{B}_\nu(\omega)$ and $\boldsymbol{C}_\nu(\omega)$ are square and invertible (29) is reduced to:

$$\begin{aligned}
\boldsymbol{G}_z(\omega) &= \boldsymbol{C}_\nu(\omega)\,\boldsymbol{\Lambda}_\nu(\omega)\,\boldsymbol{\Lambda}'^{-1}_\nu(\omega)\,\boldsymbol{C}_\nu^{-1}(\omega) - \boldsymbol{I}_\nu \\
&= \boldsymbol{C}_\nu(\omega)\,\boldsymbol{\Lambda}_\nu(\omega)\,[[\boldsymbol{I}_\nu + \boldsymbol{\Lambda}_\nu(\omega)]^{-1}\boldsymbol{\Lambda}_\nu(\omega)]^{-1}\boldsymbol{C}_\nu^{-1}(\omega) - \boldsymbol{I}_\nu \\
&= \boldsymbol{C}_\nu(\omega)\,[\boldsymbol{I}_\nu + \boldsymbol{\Lambda}_\nu(\omega)]\boldsymbol{C}_\nu^{-1}(\omega) - \boldsymbol{I}_\nu \\
&= \boldsymbol{C}_\nu(\omega)\,\boldsymbol{\Lambda}_\nu(\omega)\boldsymbol{C}_\nu^{-1}(\omega)
\end{aligned} \tag{31}$$

Thus, the ν nonzero eigenvalues of the original transfer function matrix $\boldsymbol{G}(\omega)$ are preserved by the transfer function $\boldsymbol{G}_z(\omega)$ of the reduced size and under the similarity transformation in (31). Consequently, it is possible to analyze flutter entirely based on the structural states of the aeroelastic responses without the need to sample any aerodynamic states of the responses. This is an encouraging outcome for wind tunnel or flight flutter testing in which normally only a handful of structural measurements, i.e., signals from accelerometers, are available.

6. Frequency-domain formulation

The stability formulation derived in the previous section using structural responses can be written more conveniently in frequency domain. Assume that the structural dynamic equations of motion subject to unsteady aerodynamic loads are

$$\boldsymbol{M}\ddot{\boldsymbol{q}} + \boldsymbol{C}\dot{\boldsymbol{q}} + \boldsymbol{K}\boldsymbol{q} = q_D\boldsymbol{Q}(k)\,\boldsymbol{q} \tag{32}$$

where k is the reduced frequency ($\equiv \frac{\omega b}{V_\infty}$). Analogous to the derivation of (8) and (9), we start by dividing the solution into the nominal and perturbed parts as $\boldsymbol{q} = \boldsymbol{q}_0 + \boldsymbol{\Delta q}$ where they satisfy, respectively,

$$\boldsymbol{M}\ddot{\boldsymbol{q}}_0 + \boldsymbol{C}\dot{\boldsymbol{q}}_0 + \boldsymbol{K}\boldsymbol{q}_0 - q_{D0}\boldsymbol{Q}(k)\,\boldsymbol{q}_0 = \boldsymbol{0} \tag{33}$$

$$\boldsymbol{M}\ddot{\boldsymbol{\Delta q}} + \boldsymbol{C}\dot{\boldsymbol{\Delta q}} + \boldsymbol{K}\boldsymbol{\Delta q} - q_D\boldsymbol{Q}(k)\,\boldsymbol{\Delta q} - \Delta q_D\boldsymbol{Q}(k)\,\boldsymbol{q}_0 = \boldsymbol{0} \tag{34}$$

and the nominal system is assumed to be free of flutter. From (34), we compute the transfer function from $\boldsymbol{q}_0$ to $\boldsymbol{\Delta q} = \boldsymbol{q} - \boldsymbol{q}_0$:

$$\boldsymbol{G}_q(\omega) \equiv \left[-\omega^2\boldsymbol{M} + j\omega\boldsymbol{C} + \boldsymbol{K} - q_D\boldsymbol{Q}(k)\right]^{-1}\Delta q_D\boldsymbol{Q}(k)$$

$$= \left[-\omega^2 \boldsymbol{M} + j\omega \boldsymbol{C} + \boldsymbol{K} - q_D \boldsymbol{Q}\,(k)\right]^{-1} \left[-\omega^2 \boldsymbol{M} + j\omega \boldsymbol{C} + \boldsymbol{K} - q_{D0} \boldsymbol{Q}\,(k)\right] - \boldsymbol{I}_N$$
$$\equiv \boldsymbol{T}_q\,(\omega)\, \boldsymbol{T}_{q0}^{-1}(\omega) - \boldsymbol{I}_N \tag{35}$$

Aagin, (35) requires two sets of frequency responses, $\boldsymbol{T}_{q0}\,(\omega)$ and $\boldsymbol{T}_q\,(\omega)$ at the two dynamic pressures. Taking DED of (35)

$$\boldsymbol{G}_q\,(\omega) \equiv \boldsymbol{V}_N\,(\omega)\, \boldsymbol{\Lambda}_N\,(\omega)\, \boldsymbol{W}_N^T\,(\omega) \tag{36}$$

leads to the MIMO stability as before. When the dynamic pressure is increased from q_D to $q_D + k\Delta q_D$, the new eigenvalues are obtained as:

$$[\boldsymbol{I}_N - k\boldsymbol{\Lambda}_N\,(\omega)]^{-1} k\boldsymbol{\Lambda}_N\,(\omega) \tag{37}$$

The critical dynamic pressure is then obtained as

$$q_{Df} = q_D + k_f\, \Delta q_D \tag{38}$$

where at least one of $1 - k_f \lambda_{Ni}\left(\omega_f\right)$'s vanishes. The flutter mode is the corresponding dynamic eigenmode, $\boldsymbol{v}_{Ni}\left(\omega_f\right)$ and it can be verified as follows. As before, at the flutter point (ω_f, q_{Df}) one of $\lambda_N(\omega_f)$'s diverges in (36). So, letting $\lambda_{N1}\left(\omega_f\right) \to \infty$ and multiplying both sides of the equation with $-\omega_f^2 \boldsymbol{M} + j\omega_f \boldsymbol{C} + \boldsymbol{K} - q_{Df} \boldsymbol{Q}\left(k_f\right)$ yields,

$$\begin{aligned}\Delta q_{Df} \boldsymbol{Q}\left(k_f\right) &\equiv \left[-\omega_f^2 \boldsymbol{M} + j\omega_f \boldsymbol{C} + \boldsymbol{K} - q_{Df} \boldsymbol{Q}\left(k_f\right)\right] \boldsymbol{V}_N\left(\omega_f\right) \boldsymbol{\Lambda}_N\left(\omega_f\right) \boldsymbol{W}_N^T\left(\omega_f\right) \\ &= \left[-\omega_f^2 \boldsymbol{M} + j\omega_f \boldsymbol{C} + \boldsymbol{K} - q_{Df} \boldsymbol{Q}\left(k_f\right)\right] \boldsymbol{v}_{N1}\left(\omega_f\right) \lambda_{N1}\left(\omega_f\right) \boldsymbol{w}_{N1}^T\left(\omega_f\right) + \\ &\quad \sum_{i=2}^{N} \left[-\omega_f^2 \boldsymbol{M} + j\omega_f \boldsymbol{C} + \boldsymbol{K} - q_{Df} \boldsymbol{Q}\left(k_f\right)\right] \boldsymbol{v}_{Ni}\left(\omega_f\right) \lambda_{Ni}\left(\omega_f\right) \boldsymbol{w}_{Ni}^T\left(\omega_f\right)\end{aligned}$$

Since the left-hand side is finite and $\lambda_{N1}\left(\omega_f\right) \to \infty$, we must require

$$\left[-\omega_f^2 \boldsymbol{M} + j\omega_f \boldsymbol{C} + \boldsymbol{K} - q_{Df} \boldsymbol{Q}\left(k_f\right)\right] \boldsymbol{v}_{N1}\left(\omega_f\right) = \boldsymbol{0} \tag{39}$$

Therefore, the dynamic eigenmode $\boldsymbol{v}_{N1}\left(\omega_f\right)$ is the flutter mode.

7. Summary of the flutter method based on DED

Summarizing what has been developed so far, we have established that when aeroelasticity is formulated and analyzed by splitting it into the nominal and perturbed parts and utilizing the DED, its stability is governed by exactly N (or $2N$ complex conjugate) dynamic eigenvalues and corresponding eigenmodes. The new flutter method based on the DED proceeds as follows:

1. Get the following transfer function from the frequency responses $\boldsymbol{T}_{q0}\,(\omega)$, $\boldsymbol{T}_q\,(\omega)$ obtained at two sub-critical points q_{D0} and $q_D = q_{D0} + \Delta q$, respectively:

$$\boldsymbol{G}_q\,(\omega) = \boldsymbol{T}_q\,(\omega)\, \boldsymbol{T}_{q0}^{-1}(\omega) - \boldsymbol{I}_N$$

2. Get DED of the transfer function:

$$\boldsymbol{G}_q\,(\omega_i) \equiv \boldsymbol{V}_N\,(\omega_i)\, \boldsymbol{\Lambda}_N\,(\omega_i)\, \boldsymbol{W}_N^T\,(\omega_i)$$

for selected frequencies ω_i's.

3. Check if $det\,[\boldsymbol{I}_N - k\boldsymbol{\Lambda}_N\,(\omega)] = 0$, or if $1 - k\lambda_N\,(\omega) = 0$ for any dynamic eigenvalue λ_N and scalar gain, k.

4. Get flutter solution, $\left(q_{Df},\ \omega_f,\ \boldsymbol{v}_N\left(\omega_f\right)\right)$ where the flutter mode $\boldsymbol{v}_N\left(\omega_f\right)$ is the dynamic eigenmode corresponding to $\lambda_N\left(\omega_f\right)$ for the critical k_f. The flutter dynamic pressure is $q_{Df} = q_D + k_f\, \Delta q_D$.

8. Numerical results: Goland wing in compressible flow

For demonstration of the new flutter method, we will study the Goland wing case (Goland, 1945; Meyer, 2007). This is a benchmark model that has been used and studied in aeronautical community for comparisons and validations of various structural and aeroelastic methods. It has been used in Kim (2015, 2016) for parametric model reduction of the structural dynamic and aeroelastic problems.

8.1. Structural and aerodynamic modeling

The heavy Goland wing finite element model in Fig. 3 is 4 ft in chord and 20 ft in span. It is a two-cell box structure with ribs at evenly spaced span wise stations. In the figure, the positive x direction points out the trailing edge of the wing, the positive y direction points from the fuselage out along the span of the wing, and the positive z direction is normal to the upper surface of the wing. For details of the specs and finite element modeling, see Kim (2015, 2016).

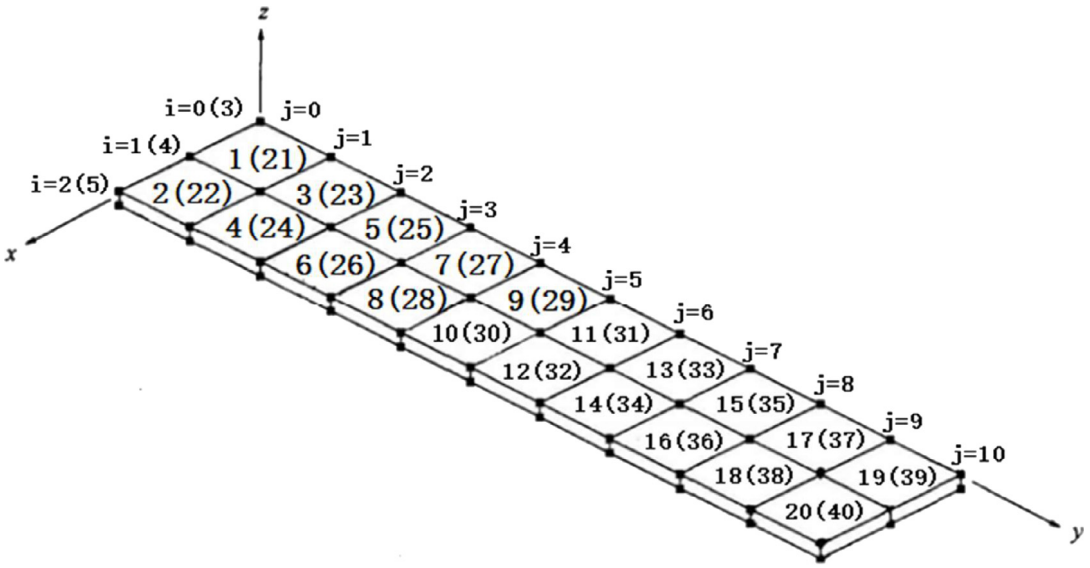

Fig. 3. Goland wing finite element model.

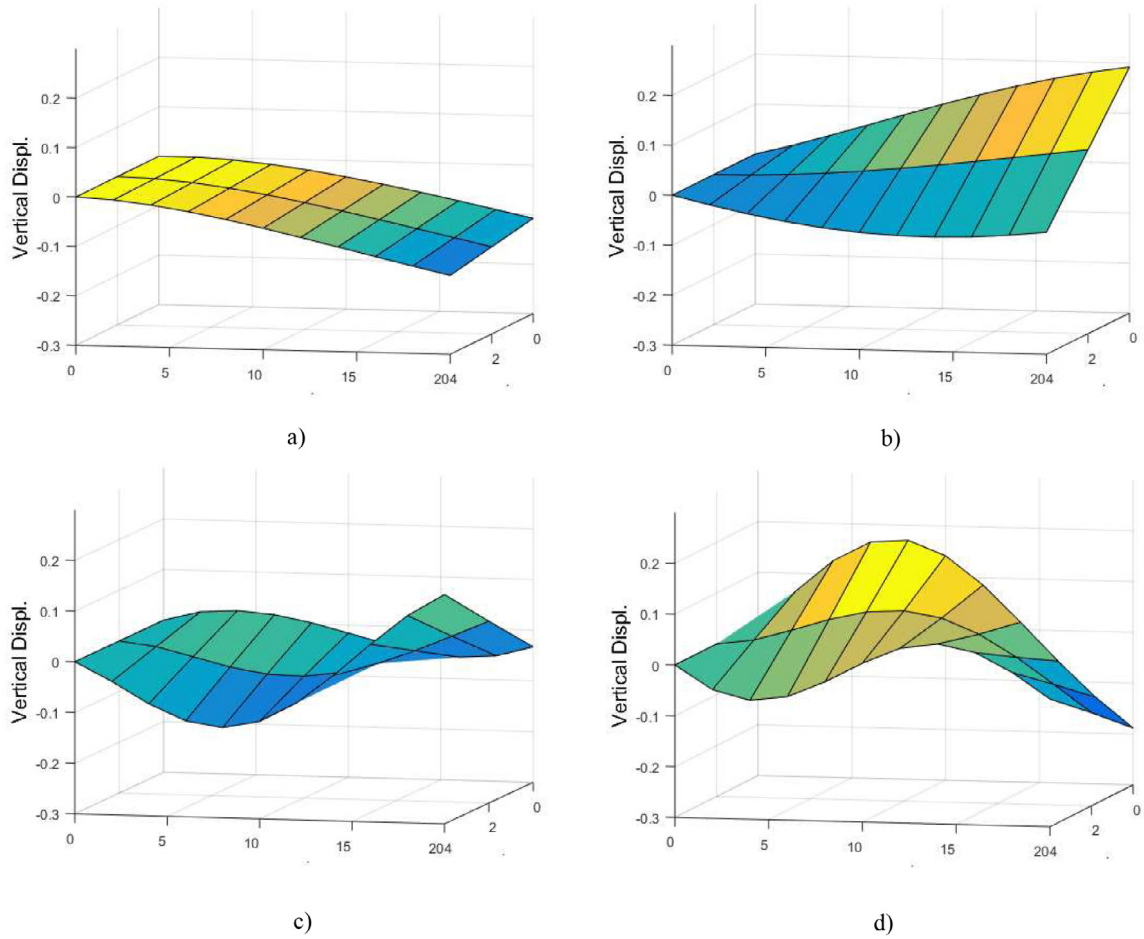

Fig. 4. Vibrational modes of Goland wing: (a) mode 1 (1.98 Hz); (b) mode 2 (4.05 Hz); (c) mode 3 (9.69 Hz); (d) mode 4 (13.49 Hz).

Fig. 4 shows the first four natural modes of the nominal wing obtained from NASTRAN (MSC Software Corp., 2012). Total of six structural modes are included in the structural model. No structural damping is assumed in the model.

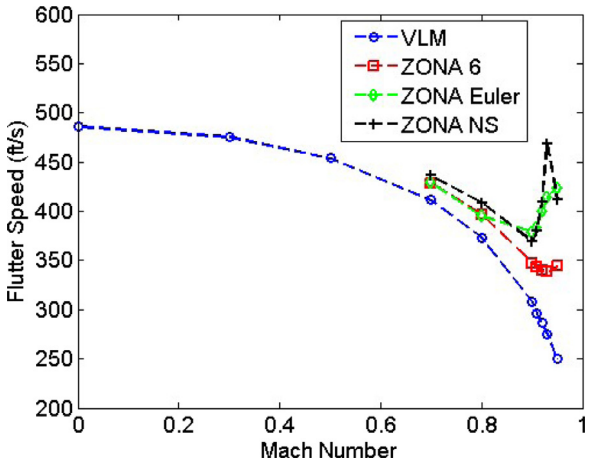

Fig. 5. Flutter boundary of the baseline Goland wing as predicted by different aerodynamic tools (Kim, 2016; Meyer, 2007).

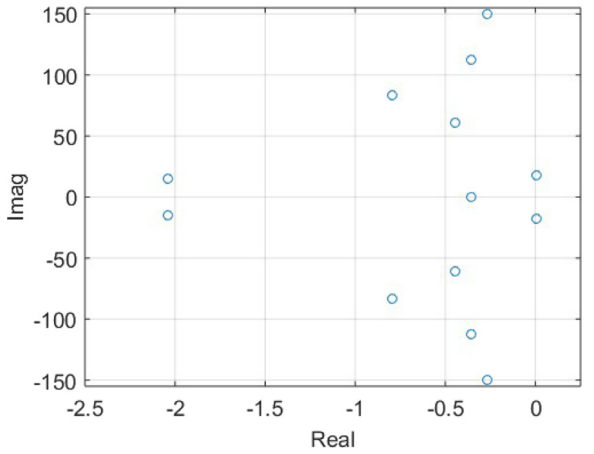

Fig. 6. Aeroelastic root loci of RFA model @ $M_\infty = .7$, $q_D = 210.5 \frac{slug}{ft\ s^2}$.

For the unsteady aerodynamics doublet lattice is used with 10, 20 panels distributed uniformly along the chordwise and span wise directions, respectively. Mach number is fixed at .7 and dynamic pressure is varied by allowing altitude to change along the constant Mach curve. As explained earlier, we will assume that the air speed is constant throughout the constant Mach curve. For Mach=.7 this speed is equal to $716.6 \frac{ft}{s} (= .7 \times 1023.7 \frac{ft}{s}$, *the mean speed of sound*). Total of 121 reduced frequencies in the range $(0, .6)$ are placed to sample the doublet lattice. This corresponds to a frequency range of $(0,\ 215)$ rad/s. During the calculation of the Nyquist plots, however, the number of frequency samples was increased to 2000 by splining the 121 aerodynamic responses. This was done to increase the resolution of the plots in the frequency domain.

8.2. Rational Function Approximation (RFA)

For a validation of the present aeroelastic modeling and analysis, the frequency valued aerodynamic loads data created by doublet lattice was converted to time domain by the Rational Function Approximation (RFA) (Roger, 1977), and an aeroelastic equation of motion was cast in the continuous-time, state-space form. For the conversion, four aerodynamic lags at $-1.0000e{-}03$, $-2.0000e{-}02$, $-7.0000e{-}02$, $-1.8000e{-}01$ were used introducing $4 \times 6 = 24$ aerodynamic lag states. The total dimension of the state-space aeroelastic equation is then 36 and flutter boundary was found by solving and checking its eigenvalues and eigenvectors of the (36×36) system matrix.

8.3. Flutter solutions at Mach=.7

For an application of the new methodology, frequency responses of the six structural coordinates were calculated and processed according to the numerical recipe summarized in Section 7. To demonstrate that flutter is an intrinsic property and

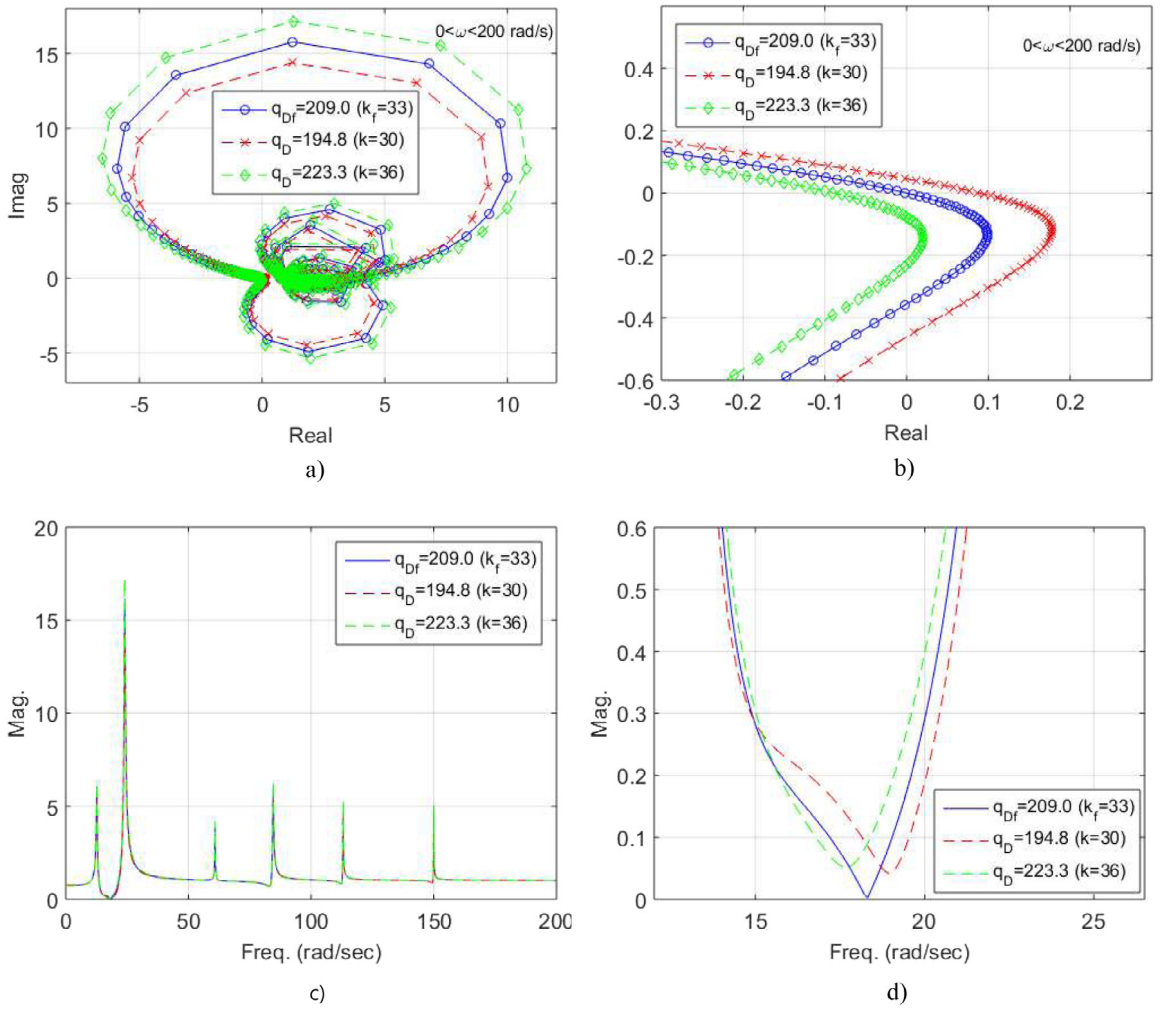

Fig. 7. Nyquist plots $det[I - k\Lambda]$ at three k values @ $M_\infty = .7, q_{D0} = .227q_{Df}, q_{D1} = .25q_{Df}$: (a) Complex; (b) Complex zoomed; (c) magnitude; (d) magnitude zoomed.

can be known from any sub-critical point below the flutter, these responses were taken at three different reference dynamic pressures and the results are compared each other. They are, $(q_{D0},\ q_{D1}) = (47.5,\ 52.25)\ ,(95,\ 104.5)\ ,(142.5, 156.75)$. For Mach=.7 based on the exact aeroelastic equation of motion Eq. (32) the wing is known to become unstable at $q_{Df} = 209$ with $\omega_f = 18.3$ rad/s. This is when the calculation is based on the CMVA and the mean air speed assumption. Thus, the three reference q_{D1}'s represent, respectively, 25%, 50%, and 75% of the known flutter dynamic pressure. Note that this flutter solution, when translated to flutter speed $V_{\infty f} = 418.4$ ft/s, is close to the results from Meyer (2007) which was obtained by assuming a fixed air density at the sea level and varying the air speed. See the flutter boundary vs. Mach plot in Fig. 5 (the dashed blue line is the flutter boundary by vortex lattice method with Prandtl-Glauert correction in the static aerodynamics). As for the RFA model it yields the flutter at $q_{Df} = 210.5$. The slight difference is due to the aerodynamic approximation necessary in the RFA procedure. See Fig. 6 for the aeroelastic eigenvalues of the RFA model at its instability condition.

The Fig. 7 shows three Nyquist plots extrapolated at $q_{D1} = 52.25$, 25% of the critical flutter dynamic pressure. They were obtained by progressively increasing the scalar gain factor k in $\boldsymbol{I}_N - k\boldsymbol{\Lambda}_N(\omega)$. For the value of $k = 30$ there is no encirclement around the zero, but for $k = 33$ the plot just touches the origin indicating that the wing is on the verge of flutter. For the increased $k = 36$ the plot clearly encircles around zero and hence it represents an unstable system. Hence, the flutter occurs at $k_f = 33$, i.e., $q_{Df} = 52.5 + k_f \Delta q = 209$. In the bottom are the same frequency responses but they are plotted against frequency. For $k_f = 33$ the frequency response touches zero magnitude at 18.3 rad/s. Hence, the flutter frequency is 18.3 rad/s. The next two figures, Figs. 8 and 9 are Nyquist plots extrapolated at $q_{D1} = 104.5, 156.75$, 50% and 75% of the critical flutter dynamic pressure, respectively. As before, for each case three different scalar gains are examined to observe how the stability changes and when the flutter occurs. For $q_{D1} = 104.5$,the critical gain value is $k_f = 11$ yielding

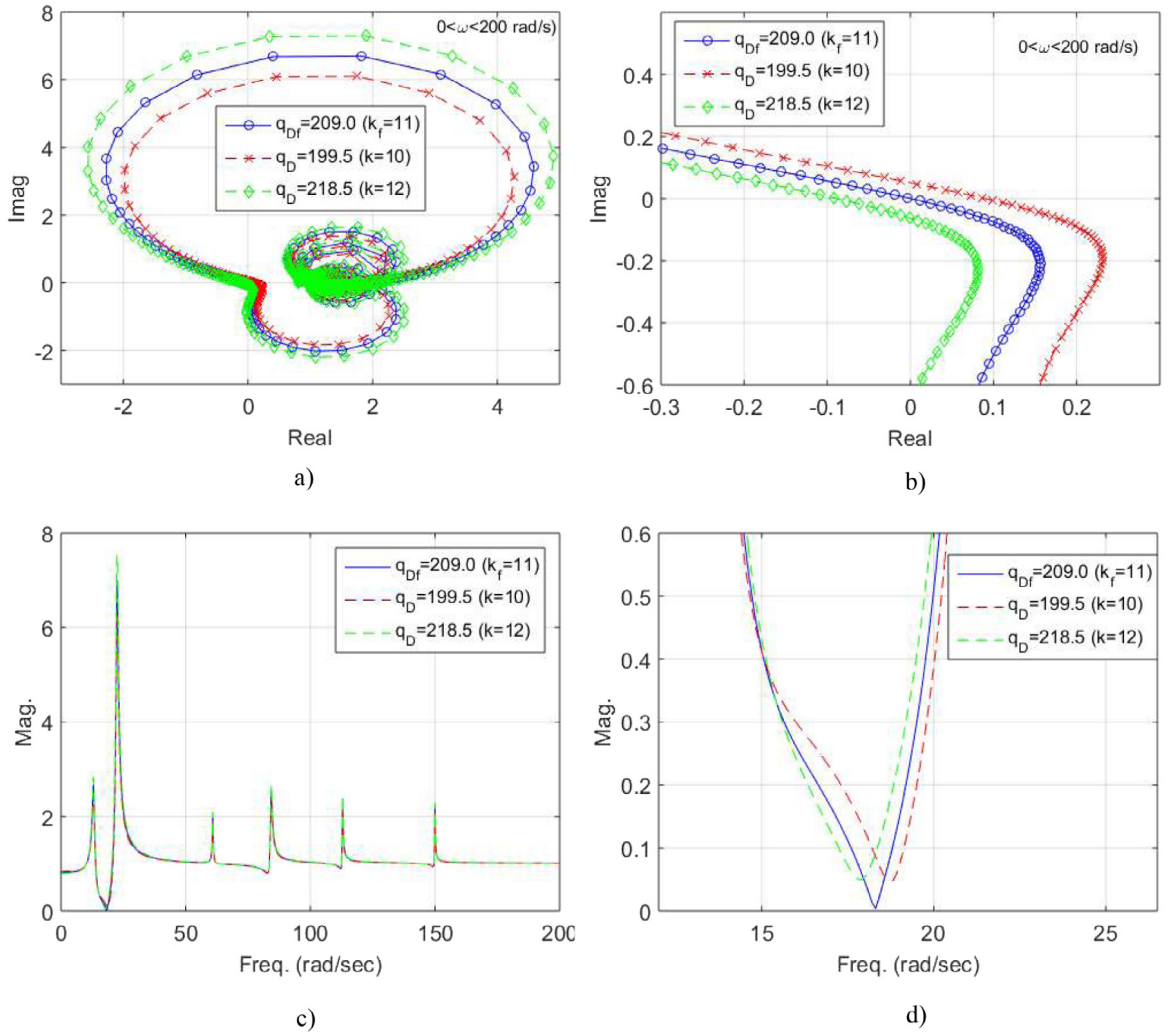

Fig. 8. Nyquist plots $det[I-k\Lambda]$ at three k values @ $M_\infty = .7$, $q_{D0} = .455q_{Df}$, $q_{D1} = .5q_{Df}$: (a) Complex; (b) Complex zoomed; (c) magnitude; (d) magnitude zoomed.

$q_{Df} = 104.5 + k_f \Delta q = 209$, while for $q_{D1} = 156.75$, $k_f = 3.67$ yielding again $q_{Df} = 156.75 + k_f \Delta q = 209$. The same can be said of the flutter frequency for which both figures agree to yield $\omega_f = 18.3$ rad/s. Therefore, it is concluded that the same flutter solution is obtained regardless at which dynamic pressure the frequency responses are taken and processed.

Fig. 10 is a dynamic eigenvalue vs. frequency that is suspected to be responsible for the flutter. Near the frequency 18.3 rad/s, $k\lambda/(1-k\lambda)$ builds up into a big spike indicating a singularity. Finally, flutter mode shape is presented in Fig. 11. This complex flutter mode is one of the dynamic eigenmodes at the critical frequency, ω_f, and corresponds to the critical dynamic eigenvalue shown in Fig. 10. As emphasized previously, this mode is independent of dynamic pressure and remains the same under all q_{D1}'s. Also plotted for a comparison is the flutter mode obtained from the RFA model. As expected, the two solutions agree extremely well. From these figures it can be seen that the flutter mode consists of mostly the first two structural modes (Fig. 4).

Lastly, to validate the assumption of the mean air speed, the flutter boundary was recalculated using the DED technique allowing an additional variation in the true air speed according to the altitude vs. speed of sound plot in Fig. 1. The new flutter point based on the matched point air speed for Mach .7 is $q_D = 209.35$. This instability occurs at $h = 30{,}640$ ft, $V_\infty = 694.33 \frac{\text{ft}}{\text{s}}$. Hence, despite the 3.1% decrease in V_∞ the critical dynamic pressure increased only by .17%. It is interesting that the current flutter dynamic pressure $q_{Df} = 209$, if it is converted to an altitude, corresponds to $h_f = 30{,}670$ ft, only 30 ft higher than the matched point solution.

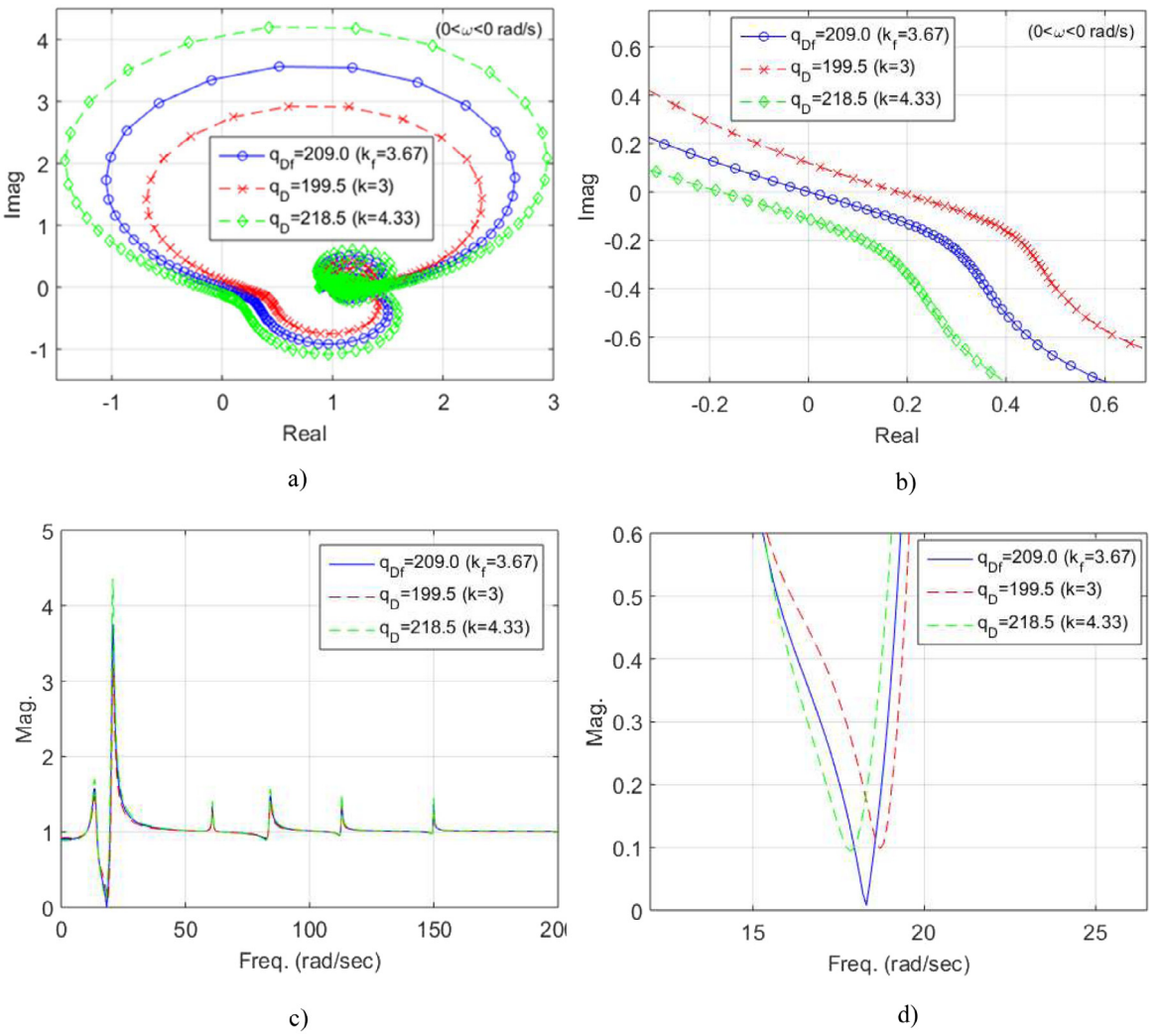

Fig. 9. Nyquist plots $det[I - k\Lambda]$ at three k values @ $M_\infty = .7, q_{D0} = .682q_{Df}, q_{D1} = .75q_{Df}$: (a) Complex; (b) Complex zoomed; (c) magnitude; (d) magnitude zoomed.

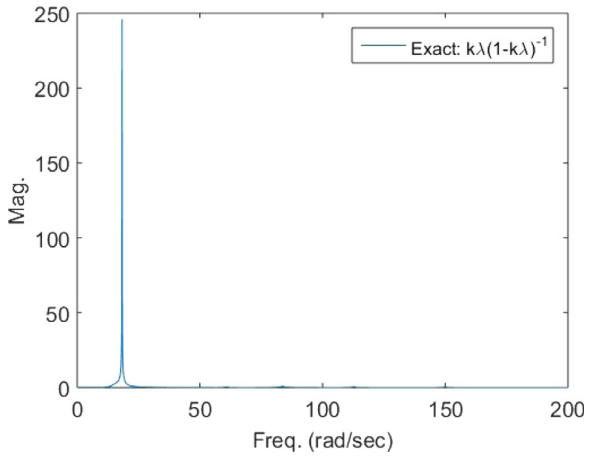

Fig. 10. $k\lambda(1 - k\lambda)^{-1}$ vs. frequency at flutter: $M_\infty = .7, q_{D0} = .455q_{Df}, q_{D1} = .5q_{Df} (k = 11)$.

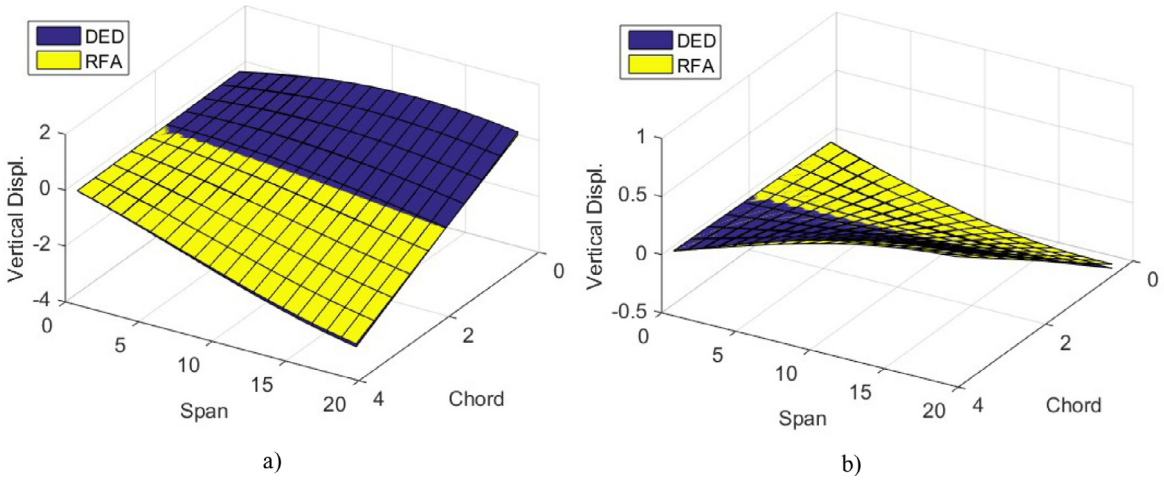

Fig. 11. Flutter mode DED vs. RFA @ $M_\infty = .7$: (a) real part; (b) imaginary part.

9. Concluding remarks

In this work, based on the idea of the Dynamic Eigen Decomposition (DED) and employing the MIMO stability criterion, a novel flutter theory and methodology have been developed. The DED leads to several key solution techniques that could be powerful in the fields of linear and nonlinear parametric modeling and reduced-order modeling, fluid–structure interaction problems, etc. The current methodology represents one of such applications feasible by the DED. It is shown that when the aeroelasticity is formulated and analyzed by splitting it into the nominal and perturbed parts and utilizing the DED, its dynamic stability is governed by exactly *2N* dynamic eigenvalues and corresponding eigenmodes of the perturbed equation, far fewer than the full dimension of the original coupled fluid–structure system. Furthermore, the dynamic eigenmodes of the aeroelastic system which contain information about the instability become invariant under dynamic pressure. This makes it possible to analyze flutter by simply extrapolating the corresponding dynamic eigenvalues through a scalar factor obtained at a low dynamic pressure. Thus, there is no need for computationally expensive and numerically sensitive algorithms such as the p–k iterations, k iterations, p iterations. Also, when used in conjunction with experimental data this approach has the potential to predict the flutter at a subcritical point below the flutter boundary and hence bodes well as a flutter testing technique. See Kim and Dowell (2018) for the latest progress in this application. In this regard and others, it should be emphasized that although derived based on the SNLDL assumption, the flutter prediction is applicable regardless of the nature of computational simulations or experimental data provided that it is possible to extract a small amplitude response by limiting the excitation to a small magnitude.

The proposed scheme was demonstrated using the Goland wing modeled by a finite element for the structure and doublet lattice for the unsteady aerodynamics. Frequency responses of the wing at two subcritical flutter points were calculated and processed to obtain the dynamic eigenmodes and dynamic eigenvalues of the aeroelastic system. It is shown that under the restriction of constant Mach and the mild assumption of the mean speed of sound the new approach yields a mathematically exact flutter solution which includes the flutter mode shape as well as the critical dynamic pressure and frequency. The method is simple to implement and can be executed efficiently in the present-day working environment, providing a powerful alternative approach to flutter calculation.

References

Goland, M., 1945. Flutter of a uniform cantilever wing. J. Appl. Mech. 12, A197–A208.
Karpel, M., 1982. Design for the active flutter suppression and gust alleviation using state-space aeroelastic modeling. J. Aircr. 19 (3), 221–227.
Kim, T., 2015. Surrogate model reduction for linear dynamic systems based on a frequency domain modal analysis. Comput. Mech. 56 (4), 709–723.
Kim, T., 2016. Parametric model reduction for aeroelastic systems: Invariant aeroelastic modes. J. Fluids Struct. 65, 196–216.
Kim, T., 2018. Higher order modal transformation for reduced-order modeling of linear systems undergoing global parametric variations. Internat. J. Numer. Methods Engrg. 1–22. http://dx.doi.org/10.1002/nme.5905.
Kim, T., Dowell, E.H., 2017. Parametrically rich nonlinear reduced-order modeling: an application in viscous incompressible flow. In: IFASD 2017, June 25–28, Como, Italy.
Kim, T., Dowell, E.H., 2018. Flutter prediction based on dynamic eigen decomposition of flight data with limited actuators and sensors. In: SciTech 2018, January 8-12, Kissimmee, FL, USA.
Maciejowski, J.M., 1989. Multivariable Feedback Design. Addison Wesley, Longman, Reading, MA.
Meyer, A.S., 2007. Variability and Model Adequacy in Simulations in Store-Induced Limit Cycle Oscillations. US Naval Academy Annapolis, MD 21402 OMB Number 074-0188.
MSC Software Corp., 2012. MSC.NASTRAN QUICK REFERENCE GUIDE.

Roger, K.L., 1977. Airplane Math Modeling Methods for Active Control Design. Structural Aspects of Active Controls, AGARD-CP-228, 4.1–4.11.
Winther, B.A., Goggin, P.J., Dykman, J.R., 2000. Reduced order dynamic aeroelastic model development and integration with nonlinear simulation. J. Aircr. 37 (5), 833–839.